Quantifying uncertainties in a Venturi multiphase configuration

Maria Giovanna Rodio, Pietro Marco Congedo

Quantifying uncertainties in a Venturi multiphase configuration

Maria Giovanna Rodio, Pietro Marco Congedo

RESEARCH REPORT
N° 8180
December 14, 2012
Project-Team Bacchus

ISSN 0249-6399 ISRN INRIA/RR--8180--FR+ENG

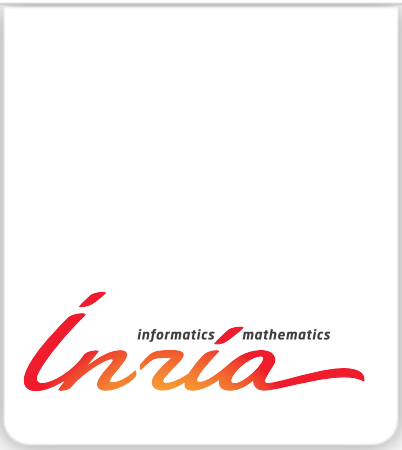

Quantifying uncertainties in a Venturi multiphase configuration

Maria Giovanna Rodio, Pietro Marco Congedo

Project-Team Bacchus

Research Report n° 8180 — December 14, 2012 — 21 pages

Abstract: Modeling the complex physical structures of cavitating flows makes numerical simulation far to be predictive, and still a challenging issue. Understanding the role of physical and parametric uncertainties in cavitating flows is of primary importance in order to obtain reliable numerical solutions. In this paper, the impact of various sources of uncertainty on the prediction of cavitating flows is analyzed by coupling a non-intrusive stochastic method with a cavitating CFD solver. The proposed analysis is applied to a Venturi tube, where experimental data concerning vapor formation are available in literature. Numerical solutions with their associated error bars are compared to the experimental curves displaying a large sensitivity to the uncertainties of inlet boundary conditions. Furthermore, this is confirmed by computing the hierarchy of most predominant uncertainties by means of an ANOVA analysis. Finally, a simple algorithm is proposed in order to provide an optimized set of parameters for the cavitation model, thus permitting to obtain a deterministic solution equal to the most probable one when considering physical inlet uncertainties.

Key-words: cavitation, uncertainty quantification, Venturi tube, polynomial chaos.

RESEARCH CENTRE
BORDEAUX – SUD-OUEST

351, Cours de la Libération
Bâtiment A 29
33405 Talence Cedex

Quantification des incertitudes dans une configuration multiphasique de type Venturi

Résumé : La modélisation des structures physiques complexes dans les écoulements cavitants diminue la capacité de prédiction de la simulation numérique. Comprendre le rôle des incertitudes physiques et du modèle devient prioritaire pour obtenir une simulation numérique robuste. Dans ce papier, l'impact des différentes sources d'incertitudes est analysé en couplant une méthode stochastique non-intrusive avec un solveur CFD pour la cavitation. L'analyse est appliquée à une configuration de type Venturi, où les données expérimentales sont disponibles en littérature. Les solutions numériques avec les barres d'erreur associées sont comparées avec les courbes expérimentales. Un algorithme simple est proposé pour calculer un ensemble de paramètres optimisé permettant d'obtenir une solution déterministe égale à la solution plus probable quand les incertitudes physiques à l'entré sont considérées.

Mots-clés : cavitation, quantification des incertitudes, configuration de type Venturi, chaos polynomial.

1 Introduction

Cavitation consists in a local pressure drop below the vapor pressure at the liquid temperature, thus creating a phase change and vapor bubbles formation. Their collapse in high-pressure region can dramatically lead to failure, erosion and other undesirable effects. For this reason, there is a strong effort devoted to develop predictive numerical tools for cavitating flows in industrial applications. Unfortunately, an accurate description of interactions between the vapour and liquid phases requires accurate physical models and a way to take into account the dynamics of the interface. Moreover, multiscale effects, turbulence and thermodynamics should be also considered.

Several numerical approaches have been proposed to reproduce cavitating flows in external and internal configurations. Principally the models can be regrouped in two major categories: interface models and two-phase models. In the first case, the liquid and the vapor phase are separated by an interface, then the systematic reconstruction of interface and the applicability to complex geometries are the most challenging issues. Concerning two-phase models, the two phases are treated as a mixture. Difficulties of these models are related to the mixture's properties estimation based on the liquid-vapor mixture ratios [1]. Differences between the various models in the second category mostly come from the relation that defines the density field. For more details concerning the various modeling approaches, Refs. [2, 3, 4] are strongly recommended. Multiphase models are derived basing on conservation principles. By the way, model is typically dependent on two types of parameters: first, on some physical parameters, such as for example the number of bubbles, that is not usually well measured; secondly, on some empiric parameters, useful for fitting and calibration procedures with respect to the experimental data. Therefore, model parameters represent an important source of uncertainty. Moreover, it is not an easy task to well define boundary and initial conditions, because of difficulties encountered in order to control accurately experiments in cavitating flows. As a result, conditions imposed for the setting of a numerical simulation, are affected by a dramatic randomness.

Actually, the numerical simulation of multiphase models is performed without considering this set of uncertainties. The numerical approach remains an useful and fundamental tool but it is hard to prove its accuracy without performing a validation with respect to the experiments, since there is no estimation of numerical solution predictivity. Finally, even if several models of different complexity exist in literature, no general consensus exists concerning the accuracy or the stability of a given model. Then, it is of primary importance in cavitating flows to determine not only a converged numerical solution but also a description of the variability of the solution with respect to the known uncertainties, *i.e.* providing the statistic moments of the quantities of interest.

In recent years, the use of stochastic methods applied to the numerical simulation in fluid mechanics is being more and more diffused. Several methods have been proposed, allowing a good estimation of statistic properties with a reduced computational cost. One of the most used methods is based on Polynomial Chaos (PC) theory first introduced by Ghanem and Spanos [5] relying on Polynomial Chaos expansion of the random variables. Intrusive [5, 6, 7, 8] and non-intrusive [9, 10, 11] formulations exist in literature, but the method used in this work is the non-intrusive spectral projection described in [12, 13].

Concerning multiphase flows, a few papers exist treating uncertainty quantification aspects. In 2000 and 2006 Li *et al.*[14] proposed a Markov stochastic model to reproduce the random behavior of cavitation bubble(s) near compliant walls. In 2003, Fariborza *et al.*[15] proposed an empirical model for the time-discrete stochastic nucleation of intergranular creep cavities. They assumed nucleation to occur randomly in time, with the temporal behavior being governed by an inhomogeneous Poisson process. In 2007, Giannadakis *et al.*[16] described the bubble breakup in

lagrangian models using a stochastic Monte-Carlo approximation. This study was oriented on the particular topic of cavitation in the Diesel nozzle holes. In 2010, Mishra *et al.*[17] introduced a model of cavitation coupled to deterministic and stochastic chemical reactions of solute chemical species.

At our knowledge, only Wilczynski [18] first and later Goel *et al.*[19] performed an uncertainties-based study on some hydrodynamic cavitation model parameters. In particular, Wilczynski [18] applied a stochastic model to capture the interaction of turbulent pressure field on cavitation nuclei population. Moreover, Goel *et al.*[19] performed a sensitivity analysis on several empirical parameters used typically in two-phase models. This study was done by means of a finite differences method. In this case, input data uncertainty characterization is not required for the sensitivity analysis, that can be performed basing only on the mathematical form of the model.

The aim of this paper consists in a systematic study for considering the probabilistic properties of the input parameters permitting to capture non-linearities in uncertainty propagation. In particular, we present a stochastic analysis, based on Polynomial Chaos method, by taking into account cavitation model parameters and physical boundary conditions uncertainties. This is applied to the numerical simulation of a cavitating flow in a Venturi configuration, that is one the most-used configuration for studying cavitation. Then, it is of great interest to assess the predictivity of cavitation model for this flow. Once computed the large variance of the most important flow properties, the second contribution of this paper is related to the formulation of a simple algorithm for improving the predictivity of the cavitation model.

This paper is organized as follows. Section 2 presents the governing equations for reproducing cavitation and the associated numerical methods for solving the deterministic and stochastic solutions. In Section 3, the Venturi configuration is described and the numerical solution is verified and validated with respect to the experimental data. Moreover, the sources of uncertainties are introduced. Then, in Section 4, stochastic analysis is presented, where the influence of uncertainties is displayed in terms of mean, variance for some quantities of interest. The most predominant uncertainties are determined with a cross-validation considering the whole set of uncertainties or different sources of uncertainties separately. Finally, in Section 5, an inverse method is briefly described permitting to provide new, more robust parameter for the cavitation model in order to obtain more reliable numerical solutions. Some conclusions and perspectives are drawn in section 6.

2 Governing equations and Numerical methods

2.1 Governing equations and Numerical Flow Solver

The numerical simulations are performed by means of the commercially available code FLUENT (release 12.0.16). For a basic two-phase cavitation model, Fluent solves the set of Reynolds-averaged Navier-Stokes (RANS) equations governing the transport of mixture, coupled with a conventional turbulence model. An implicit finite volume scheme based on a segregated Pressure-Based Solver (SIMPLE algorithm for the pressure-velocity coupling) is used, with a 2nd order upwind differentiating scheme, except for pressure and vapor fraction where a standard and a 1st order upwind schemes are used, respectively.
First, let us introduce the mass and momentum equations for the mixture as follows:

$$\frac{\partial \hat{\rho}}{\partial t} + \frac{\partial \hat{\rho}\hat{u}_i}{\partial x_j} = 0 \tag{1}$$

$$\frac{\partial \left(\hat{\rho}\hat{u}_i\right)}{\partial t} + \frac{\partial \left(\hat{\rho}\hat{u}_i\hat{u}_j\right)}{\partial x_j} = -\frac{\partial \left(\hat{p}\right)}{\partial x_i} + \frac{\partial}{\partial x_j}\left[\left(\mu+\mu_t\right)\left(\frac{\partial \hat{u}_i}{\partial x_j} + \frac{\partial \hat{u}_j}{\partial x_i} - \frac{2}{3}\delta_{ij}\frac{\partial \hat{u}_k}{\partial x_k}\right)\right] + \hat{\rho}g \tag{2}$$

where i, j and k denote the axes coordinate, t is the time, $\hat{\rho} = \alpha\rho_v + (1-\alpha)\,\rho_l$ is the mixture density where v and l indicate the vapor and liquid phase, respectively, and α is the vapor volume fraction. The term $\hat{u}$ represents the mixture velocity, where the slip velocity is assumed to be equal to zero, $\hat{p}$ is the mixture pressure, g is the gravity acceleration, $\mu_m = \alpha\mu_v + (1-\alpha)\,\mu_l$ and $\mu_{m,t}$ are the mixture viscosity and turbulent mixture viscosity, respectively. This last one is a function of both the turbulent kinetic rate k and the turbulence dissipation rate ϵ:

$$\mu_{m,t} = \hat{\rho} C_\mu \frac{k^2}{\epsilon} \tag{3}$$

where C_μ is a constant (see Tab. 1).

As a consequence, two additional transport equations for k and ϵ are needed:

$$\frac{\partial\left(\hat{\rho}k\right)}{\partial t} + \nabla\cdot\left(\hat{\rho}k\vec{\hat{u}}\right) = \nabla\cdot\left(\frac{\mu_{m,t}}{\sigma_k}\nabla k\right) + G_{m,k} - \hat{\rho}\epsilon \tag{4}$$

$$\frac{\partial\left(\hat{\rho}\epsilon\right)}{\partial t} + \nabla\left(\hat{\rho}\epsilon\vec{\hat{u}}\right) = \nabla\cdot\left(\frac{\mu_{m,t}}{\sigma_\epsilon}\nabla\epsilon\right) + \frac{\epsilon}{k}(C_{1\epsilon}G_{m,k} - C_{2\epsilon}\hat{\rho}\epsilon) \tag{5}$$

where $G_{m,k} = \mu_{m,t}(\nabla\vec{\hat{u}} + \nabla\vec{\hat{u}}_t) : \nabla\vec{\hat{u}}$ represents the generation of turbulence kinetic energy, due to the mean velocity gradients, $C_{1\epsilon}$ and $C_{2\epsilon}$ are two constants, σ_k and σ_ϵ are the turbulent Prandtl numbers for k and ϵ, respectively.

Two terms are assumed as negligible in Eq. (4) and (5): i) the term of turbulence kinetic energy generation (due to the buoyancy because of tiny liquid temperature variation); ii) the contribution of the fluctuating dilatation in compressible turbulence to the overall dissipation rate, because the flow is incompressible.

Constants values are provided for water in table 1 (see [20] for more details). The near-wall region is modeled by a *wall function* that links the viscosity-affected region between the wall and the fully-turbulent region. A named *standard wall function*, based on the work of Launder and Spalding [21], is used in this paper.

Table 1: Values of constants for water

$C_{1\varepsilon}$	$C_{2\varepsilon}$	C_μ	σ_k	σ_ε
1.44	1.92	0.09	1.0	1.3

The cavitation is taken into account by using the Schnerr and Sauer model [22, 23], *i.e.* a transport equation with a source term for the vapor phase (v):

$$\frac{\partial\alpha\rho_v}{\partial t} + \nabla\cdot\left(\alpha\rho_v\vec{\hat{u}}\right) = \dot{m}_e + \dot{m}_c = \frac{\rho_v\rho_l}{\rho}\frac{D\alpha}{Dt}, \tag{6}$$

where $\dot{m}_e$ and $\dot{m}_c$ describe the mass transfer for evaporation and condensation, respectively. In order to close the system, it is necessary to introduce a relation for the volume fraction α. It can be defined as:

$$\alpha = \frac{\frac{4}{3}\pi\eta R^3}{\left[1 + \frac{4}{3}\pi\eta R^3\right]}, \tag{7}$$

where R is the bubble radius and η is the nuclei concentration per unit of pure liquid volume. In this work, η is assumed equal to a constant, considering that no bubbles are created or destroyed. A simplified Rayleigh-Plesset equation [24] is introduced in order to model the bubble radius R:

$$\frac{DR}{Dt} = \sqrt{\frac{2}{3}\frac{p_b - p}{\rho_l}}, \tag{8}$$

where D/Dt is the material derivative, p_b is the bubble pressure, p is the pressure far from the bubble that is assumed to be equal to $\hat{p}$.

Finally, the complete system is defined by eight equations (Eqs. (1), (2), (4), (5), (6), (7), (8)) with eight unknowns $(\hat{\rho}, \hat{u}, \hat{p}, p_b, R, k, \epsilon)$. Remark that the cavitation model depends only on one parameter, *i.e.* the nuclei concentration per unit of pure liquid volume η.

The quantities $\dot{m}_e$ and of $\dot{m}_c$ related to the Schnerr and Sauer model [22, 23] can be obtained by coupling Eqs. (6, 7, 8) as follows:

$$\dot{m}_e = \frac{\rho_v \rho_l}{\rho} \alpha(1-\alpha) \frac{3}{R} \sqrt{\frac{2}{3} \frac{p_b - p}{\rho_l}} \ \ when \ \ p_b > p \tag{9}$$

and

$$\dot{m}_c = \frac{\rho_v \rho_l}{\rho} \alpha(1-\alpha) \frac{3}{R} \sqrt{\frac{2}{3} \frac{p - p_b}{\rho_l}} \ \ when \ \ p_b \leq p. \tag{10}$$

2.2 Stochastic Method

Let us consider a stochastic differential equation of the form:

$$L\left(\mathbf{x}, \theta, \phi\right) = f\left(\mathbf{x}, \theta\right) \tag{11}$$

where L is a non-linear spatial differential operator (for istance, L is the steady Navier-Stokes operator) depending on a random vector θ (whose dimension depends on the number of uncertain parameters in the problem) and $f(\mathbf{x}, \theta)$ is a source term depending on the position vector $\mathbf{x}$ and on θ. The solution of the stochastic equation (11) is the unknown dependent variable $\phi(\mathbf{x}, \theta)$, and is a function of the space variable $\mathbf{x} \epsilon \mathbf{R}^d$ and of θ. Under specific conditions, a stochastic process can be expressed as a spectral expansion based on suitable orthogonal polynomials, with weights associated with a orthogonal polynomials, with weights associated with a particular probability density function. The first study in this field is the Wiener (1938) process. The basic idea is to project the variables of the problem onto a stochastic spaceproject the variables of the problem onto a stochastic space spanned by a complete set of orthogonal polynomials Ψ that are functions of random variables $\xi\left(\theta\right)$, where θ is a random event. For example, the unknown variable ϕ has the following spectral representation:

$$\phi\left(\mathbf{x}, \theta\right) = \sum_{i=0}^{\infty} \phi_i\left(\mathbf{x}\right) \Psi_i\left(\xi\left(\theta\right)\right) \tag{12}$$

In practice, the series in Eq. (12) has to be truncated to a finite number of terms, here denoted with N. The total number of terms of the series is determined by:

$$N + 1 = \frac{(n + p_0)!}{n!\ p_0!} \tag{13}$$

where n is the dimensionality of the uncertainty vector θ and p_0 is the order of the polynomial expansion. Substituting the polynomial chaos expansion (12), into the stochastic differential equation (11) yields:

$$L\left(\mathbf{x}, \theta; \sum_{i=0}^{N} \phi_i\left(\mathbf{x}\right) \Psi_i\left(\xi\left(\theta\right)\right)\right) = f\left(\mathbf{x}, \theta\right) \tag{14}$$

Equation (14) is solved through the weighted residual method. The collocation method is obtained by choosing Dirac-delta weighting functions. The coefficients $\phi_i\left(\mathbf{x}\right)$ are obtained using

quadrature formulae based on tensor product of a 1D formula. Applying a collocation projection to equation (14), we obtain the solution of a deterministic problem for each collocation point. For further details, see Congedo *et al.*[13]. In both cases, once the chaos polynomials and the associated ϕ_i coefficients are computed, the expected value and the variance of the stochastic solution $\phi_i(\mathbf{x}, \theta)$ are obtained from :

$$E_{PC} = \phi_0(\mathbf{x}) \tag{15}$$

$$Var_{PC} = \sum_{i=0}^{N} \phi_i^2(\mathbf{x}) \left\langle \Psi^2 \right\rangle \tag{16}$$

Another interesting property of PC expansion is to make easier sensitivity analysis based on the analysis of variance decomposition (ANOVA). ANOVA allows identifying the contribution of a given stochastic parameter to the total variance of an output quantity. It can be easily computed by using some interesting properties of the previous development [12]. Let us recall here that the contribution to the variance of a given random variables with index i, *i.e.* the first order Sobol's index, can be obtained by:

$$S_i = \frac{\sum_{\alpha \geq i} \phi_i^2(\mathbf{x}) \left\langle \Psi^2 \right\rangle}{Var_{PC}} \tag{17}$$

For more details, Ref. [12] is strongly recommended.

2.3 Coupling CFD and uncertainty quantification tool

Non-intrusive stochastic method, presented in the previous section, allows reducing the stochastic problem into a series of deterministic runs where specific values for parameters affected by uncertainties are considered. Then, the CFD solver is not modified and it remains completely decoupled from the stochastic code. Once deterministic runs performed, they are used to compute statistics of the solution by means of equations (15) and (16). Results presented here are obtained by considering various order of polynomial chaos.

3 Venturi configuration

Venturi configuration is one the most popular system for studying cavitation from numerical and experimental point of view. In particular, the section chosen for this study has been designed to reproduce cavitating flows developing on the blades of space turbopump.

3.1 Case description and available experimental data in literature

We have focused our attention to the experimental results of the Venturi test section of the CREMHYG (Centre dâĂŹEssais de Machines Hydrauliques de Grenoble) [25]. It is constituted of a profile with a convergence angle of 4.3 degree and a divergence angle of 4 degree, equipped with five probing holes to measure the local void ratio, instantaneous local speed and pressure. A schematic representation of the tunnel and of probes position is reported in figure 1, while a detailed description of the experimental device is given in [25] and in [26]. The fluid used in this experiment is water (the physical parameters are reported in table 2). The test case operating conditions (summarized in table 3) yield an experimental cavity length L between 70 mm and 85 mm.

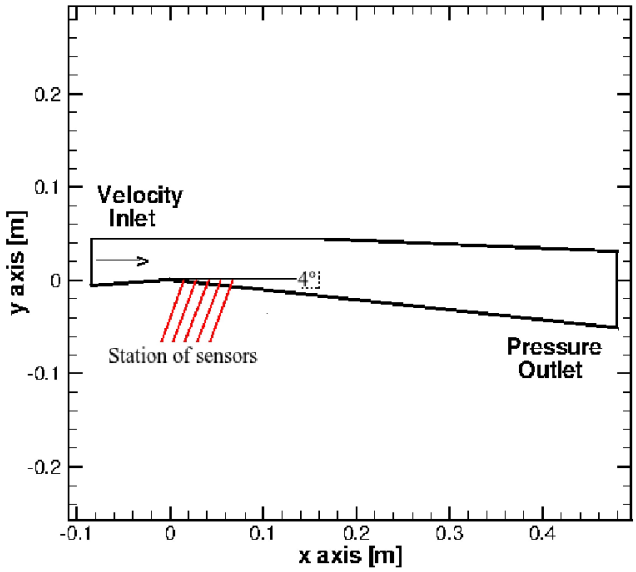

Figure 1: Schematic representation of Venturi test section

Table 2: Physical parameters for water

$T\ [K]$	$\rho_v\ [kg/m^3]$	$\rho_l\ [kg/m^3]$	$P_v\ [Pa]$
293	0.0173	998	2339

Table 3: Test case operating conditions

$V_{inlet}\ [m/s]$	$Q\ [m^3/s]$	$P_{inlet}\ [Pa]$	$P_{outlet}\ [Pa]$
10.8	0.02375	36000	21000

3.2 Verification and validation of the numerical solution

First, a grid convergence study is performed following RoacheâĂŹs method [27] based on Richardson extrapolation. This method allows estimating the real scheme's order of convergence that is lower than theoretical order of convergence of numerical algorithm utilized. The order of convergence p can be obtained handling three numerical solutions computed on grids of increasing density, with constant grid-refinement ratio r :

$$p = ln\left[\frac{f_3 - f_2}{f_2 - f_1}\right] / ln\,(r) \tag{18}$$

where f is a solution functional and indices 1 and 3 are referred to the finer and the coarser grid solution, respectively. For the present computations, we consider H-type mesh, where the coarse, the medium and the fine grid present, respectively, 23541, 94164 and 376656 cells. A zoom near the Venturi throat for the fine grid is reported in Fig. 2. The order of convergence

p is computed in a point in the cavitating region, between the thoat and the wall. For the present computation, p is computed on the flow pressure and velocity and, respectively, we have calculated a value of 1.5 and 1.9 against a theoretical order of convergence of 2. The value of p is important in order to choose the grid that assures a good tradeoff between the solution accuracy and the computational cost. Moreover, we compute the grid convergence index (GCI) on the finer and medium grid. It represents an estimate of how far the numerical solution is from its asymptotic value. We compute GCI values of 0.02% (0.055%) for static pressure and 0.26% (0.99%) for the velocity when a finer (medium) grid is used, indicating that the solution is well within the asymptotic range. Moreover, in Fig. 3, results in terms of velocity and void ratio are reported for the three grids at the station 1. It can be observed that medium and fine grids display very similar results. Basing on these considerations, the medium grid has been chosen for all the subsequent simulations.

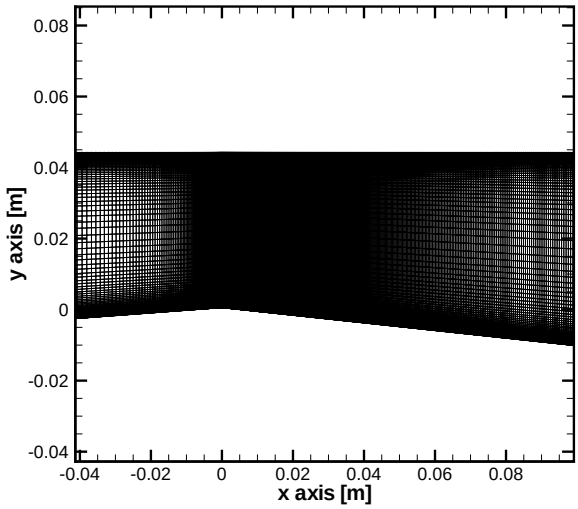

Figure 2: Zoom of the fine grid near the Venturi throat

In Fig. 4, the deterministic void fraction and velocity profiles obtained with the Schnerr model at three stations, are plotted with the best solution shown in [25] and with the experimental data. There is a good agreement between experimental and deterministic results obtained with the Schnerr Model in terms of void ratio at station 1 and 2 when $y > 0.0035$ m. On the opposite, differences between experiments and computation are observed when $y < 0.0035$ m, displaying a maximal error of 200% at $x = 0$ m as in Barre *et al.*. At station 3, the deterministic solution does not shown void fraction ($alpha$=0) that correspond an error of 100% at y=0.003 m, even if the solution is better than the estimation in Barre *et al.*. On the contrary, for the velocity, we can observe a good agreement between experimental and deterministic results (Schneer Model) at station 2 and 3, better than the computation of Barre *et al.* that, on the opposite, shows a better agreement at station 1. The Fig. 5 represents the mean wall pressure longitudinal evolution. The numerical prediction fits with measurements in the first part of divergent ($0 < x < 0.07$) as well as in the part where the experimental results indicate a more rapid recompression process.

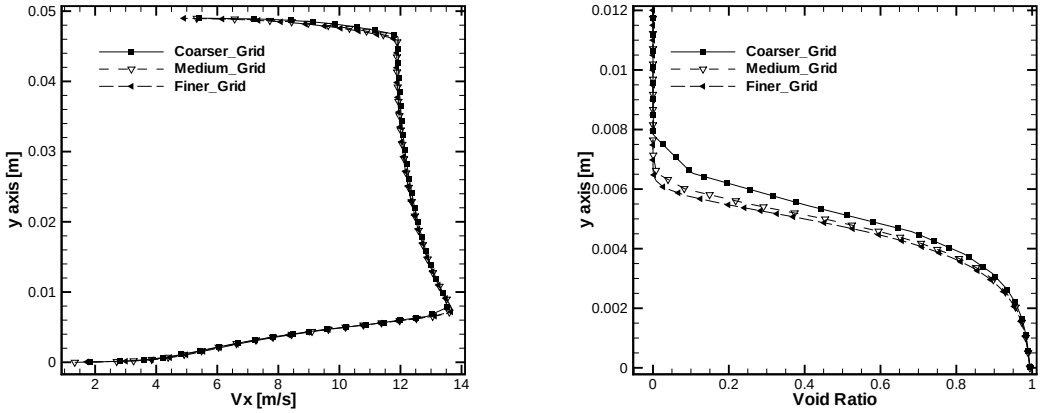

(a) Station 1 (b) Station 1

Figure 3: Velocity profiles and void fractions at the station 1 for the three grids used in the mesh convergence study

3.3 Sources of uncertainty

In Barre [1], physical measurements are provided with their estimated errors at the inlet flow and at the five stations where probes are present. These estimations have been used in this paper in order to compare experimental error bars with those one computed by means of stochastic simulations. Then, the following experimental errors have been taken into account: $\pm 0.25\%$ for the inlet flow rate, ± 0.05 $[bar]$ for the inlet pressure, ± 19 $[Pa]$ for the pressure at different stations, $\pm 15\%$ for the void ratio at different stations.

As already explained in 2.1, cavitation model is affected globally by one uncertainty on n. Moreover, experimental uncertainties on inlet conditions (pressure and velocity) have been taken into account. Then, globally, three uncertainties are considered in the stochastic simulation. The mean values, maximal variations and pdf type for each parameter are summarized in next table. Seeing that an accurate estimation of probability density function for the physical measures, used as input parameters in the numerical simulation, is not available, we used sistematically uniform pdf. This choice represents a robust safety strategy in order to analyse uncertainty propagation of physical uncertainties. Concerning modelling uncertainty, this epistemic (*i.e.* due to a lack of knowledge) variable is treated again as a uniform pdf, that is one of the possible options when considering this kind of uncertainty.

Table 4: Mean values, maximal variation and probability density function (PDF) for model and operating conditions uncertainties

		Mean values	Max variations	PDF
n	Decoupled/Coupled	10^{10}	$\pm 10^5$	Uniform
p	Decoupled/Coupled	$36000\,[Pa]$	$\pm 5000\,[Pa]$	Uniform
v	Decoupled/Coupled	$10.8\,[m^3/s]$	$\pm 0.025\%$	Uniform

4 Stochastic analysis

4.1 General strategy

The analysis of the contribution of the three uncertainties to the variance of the outputs of interest (vapor fraction, velocity and pressure) is first performed following a decoupled analysis: a single source of uncertainty is taken into account, the other source being held constant equal to the respective mean values. This analysis is carried out with several orders of PC, using a full tensorization for the choice of collocation points. The L2 norm for the mean and the variance of pressure are computed when uncertainties on the input and on the model are taken into account (the 5th order of polynomial chaos is taken as reference). Convergence curves are reported in figure 6. As it can be seen, the stochastic solutions are well converged for an order equal to 3. Results obtained with this decoupled analysis are resumed in figure 7, where radial vapor distributions with error bars at different sections are reported. Except at the station 1, uncertainty propagation due to the inlet uncertainties is much more strong than that one related to model uncertainty. Let us focus on the inlet uncertainties results (figure 7(a,c,e)): experimental bars are well inside the numerical error bars at station 5. At station 3, this happens only for $y > 0.003$. At station 1, numerical error bars are more tiny than the experimental ones.

In a second step, all the sources of uncertainty (modelling and inlet conditions) are simultaneously taken into account in order to assess possible interactions between the model and the operating conditions that might contribute to the variance of void fraction. Decoupled and coupled analysis are used in order to cross-validate statistic estimations. Convergence curves for the coupled analysis are reported in figure 6. Also in this case, stochastic solution are well-converged for a polynomial chaos order equal to 3. Mean and variance contours in the flowfield are computed for vapor fraction, for velocity and pressure, that are reported in figures 8, 9 and 10, respectively. For the three variables, variance is maximal near the wall. Finally, in figure 11, radial vapor (a,c,e) and velocity (b,d,f) distributions with error bars at different sections are reported. The same qualitative conclusions derived from the decoupled uncertainties are confirmed in this case: at stations 3 and 5, experimental error bars are included in the numerical bars, while at station 1, larger differences are observed between the numerical and experimental curves.

5 Setting of optimized parameters for the cavitation model

When experimental data are not available, the use of UQ techniques could be of great interest in order to set up some empirical parameters, usually treated like epistemic uncertainties. Instead of running every time a stochastic problem, the computation of an optimized empirical parameter could allow to obtain a solution very similar to the most probable one by running only a deterministic simulation.

Let us focus on our case of study. The cavitation model is affected by an epistemic uncertainty on n, while aleatory uncertainties caracterize the inputs. It could be useful to optimize the value of n permitting to obtain in a deterministic framework, the most probable (in a stochastic sense) solution. This could be a general approach for optimizing epistemic uncertainties basing on the aleatory uncertainties, when experiments are not available.

Remark that the optimized value do not permit a-priori to reproduce better experimental results but the idea is to give the most probable solution basing on the chosen multiphase model. In this way, when comparing with experiments, some more definitive conclusions can be drawn in terms of predictivity of the model without conditionating the results making some arbitrary calibration of the model. This is faster with respect to a bayesian calibration and do not require

experimental data.

The objective of the study is to find optimal model parameters ensuring that the associated simulation be equal to the most probable solution when considering uncertainties on inlet conditions. Using the notations introduced in the previous section, this *problem* to solve can be mathematically expressed as:

$$\min_{\boldsymbol{n}} \sum_{j} \left\| \mu_{\mathrm{u}_j} - Q_j(n) \right\| \tag{19}$$

where μ_{u_i} is computed with respect to the inlet uncertainties. The quantity Q denotes the field value obtained in the cell j when the model parameter n is used, and $\|\boldsymbol{\xi}\|$ is a L2-norm.

The problem defined by Eq. (19) is a particular optimization problem. The output of interest is the vapor fraction. An optimized value of n equal to $10^{10.1309}$ is obtained, permitting to obtain the most probable solution using a deterministic approach with an error of 0.1%.

6 Conclusion and Future Work

In this paper, we performed a stochastic analysis of a cavitating flow evolving in a Venturi configuration. Main results of this analysis are the following:

- The cross-validation between decoupled and coupled analysis and ANOVA results display similar qualitative behaviors in terms of the computation of most predominant uncertainties.
- A third order of the polynomial chaos expansion is sufficient to attain convergence over all the flowfield for the pressure and the vapor fraction.
- Experimental uncertainties on inlet boundary conditions are predominant with respect to the model-uncertainty. The meaning of this analysis is twofold: first, the choice of the model seems to be less important when inlet uncertainties are strong; secondly the predictivity of the numerical simulation of cavitating flows seems questionable since the large variation of the vapor fraction.

Finally, we proposed a very simple algorithm for using the stochastic solution in order to get some optimized parameter related to the epistemic uncertainty. The idea is to use this optimized parameter for obtaining the most probable solution only by running a deterministic simulation. Different configurations will be investigated in a future work.

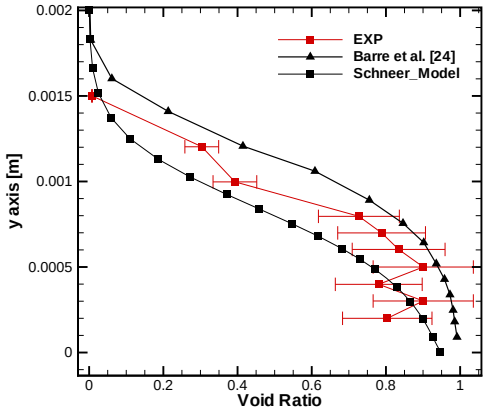

(a) Station 1

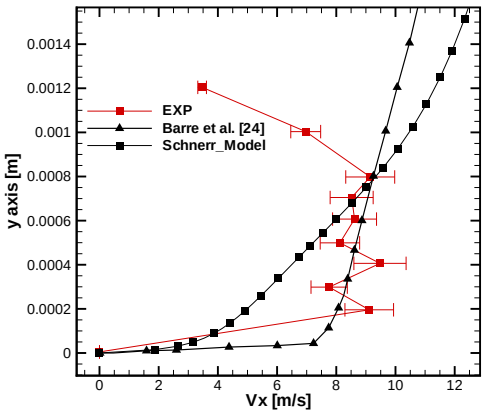

(b) Station 1

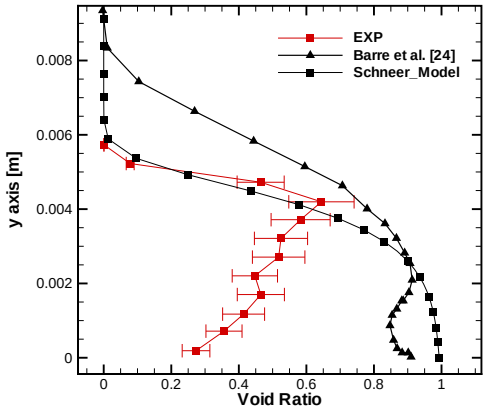

(c) Station 3

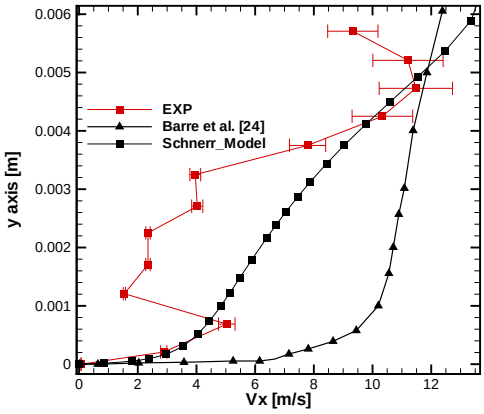

(d) Station 3

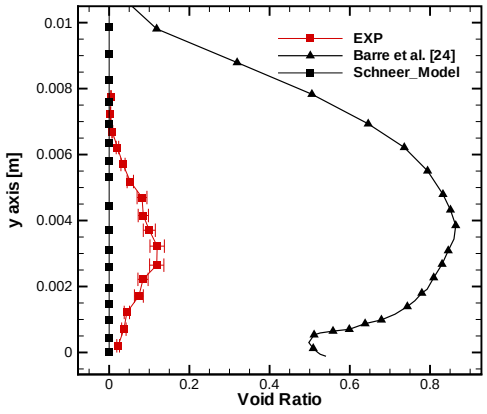

(e) Station 5

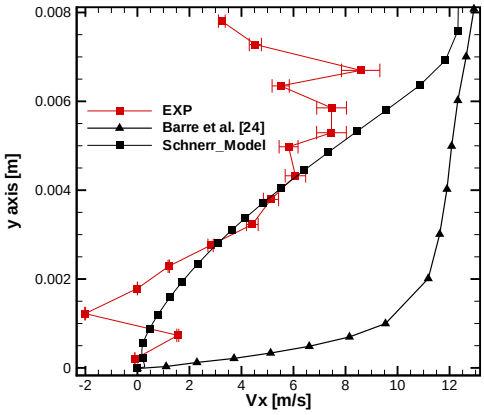

(f) Station 5

Figure 4: Radial vapor (a,c,e) and velocity (b,d,f) distributions. Comparison with results shown in [25] and experimental measurements at different sections.

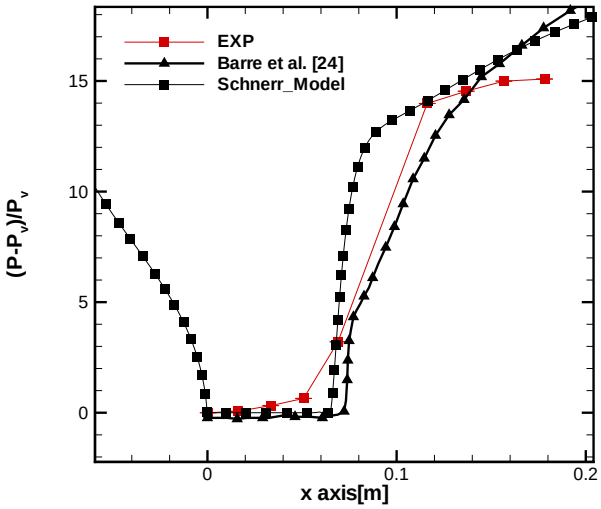

Figure 5: Longitudinal mean wall pressure evolution

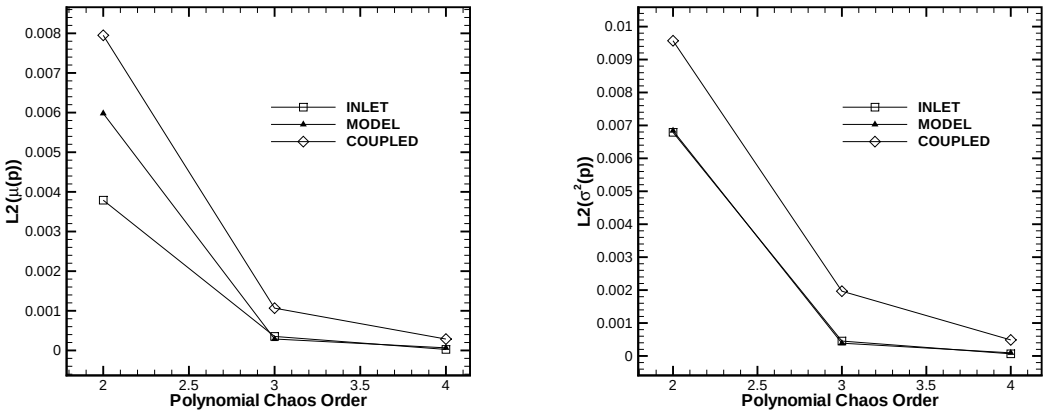

Figure 6: Convergence curves for the mean (left) and the variance (right) of the pressure in the flowfield. A L2 norm is used.

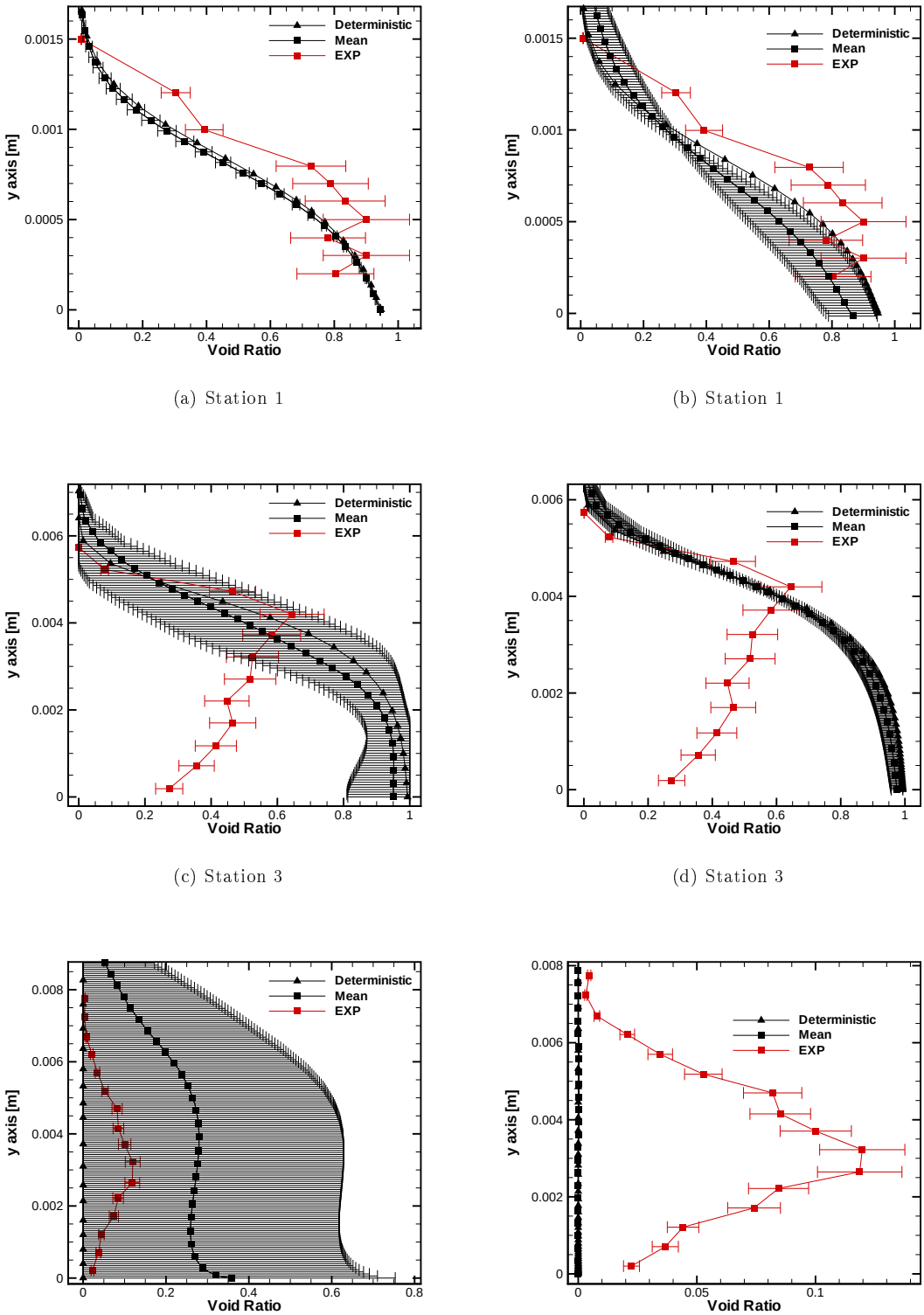

(a) Station 1

(b) Station 1

(c) Station 3

(d) Station 3

(e) Station 5

(f) Station 5

Figure 7: Radial vapor distributions with error bars at different sections when decoupled uncertainties are considered: uncertainties on inlet conditions (a,c,e) and on the model (b,d,f). The results are compared with experimental measurements

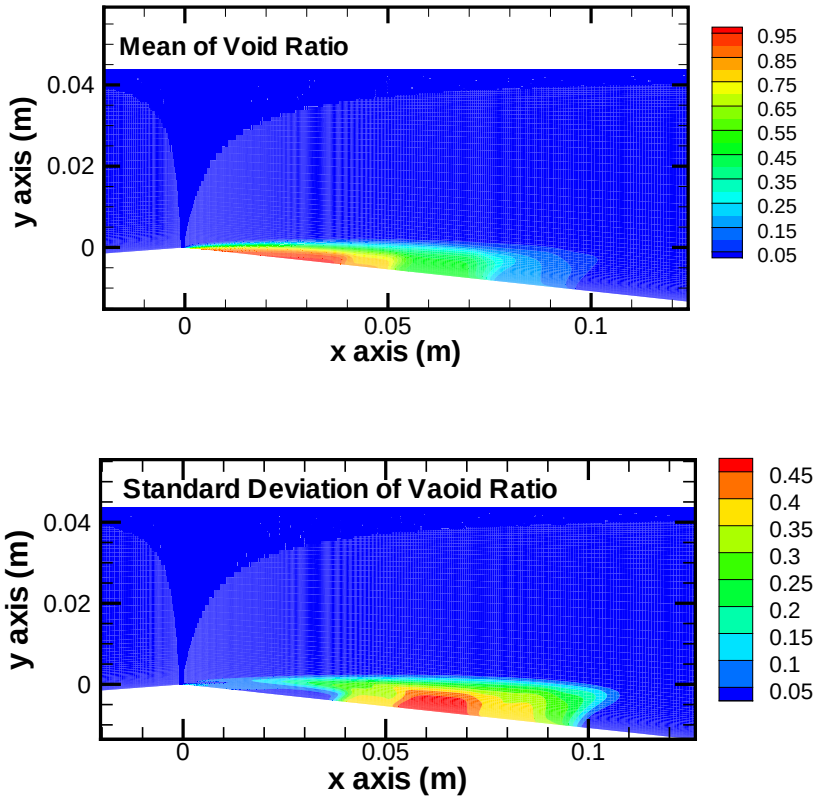

Figure 8: Contour of mean (top) and variance (bottom) of the vapor fraction in the flowfield. The whole set of uncertainties is taken into account.

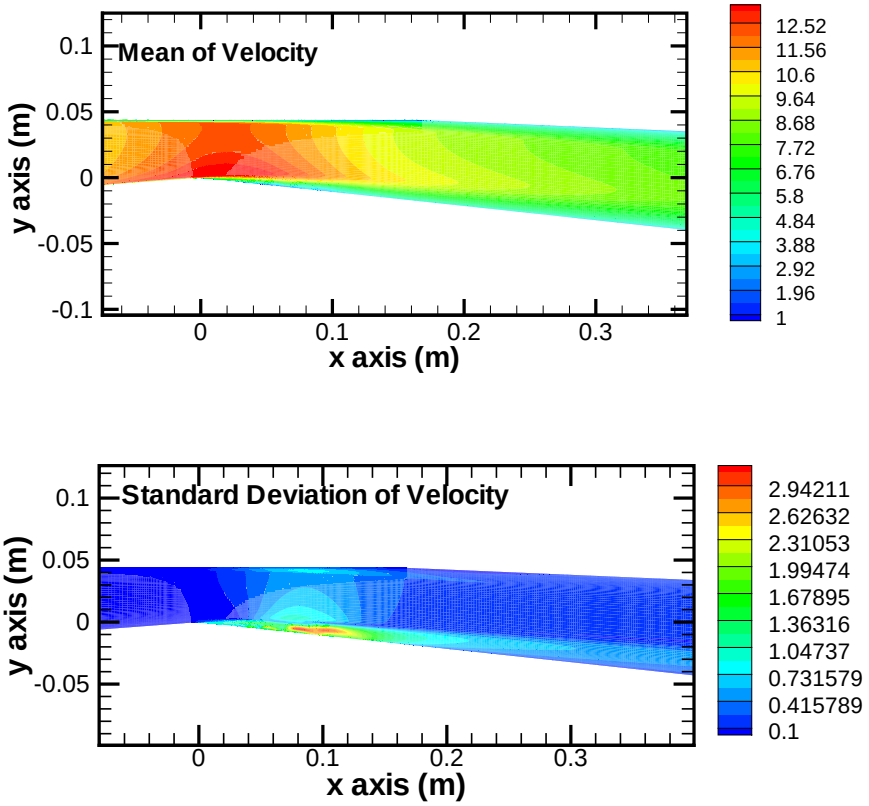

Figure 9: Contour of mean (top) and variance (bottom) of the velocity in the flowfield. The whole set of uncertainties is taken into account.

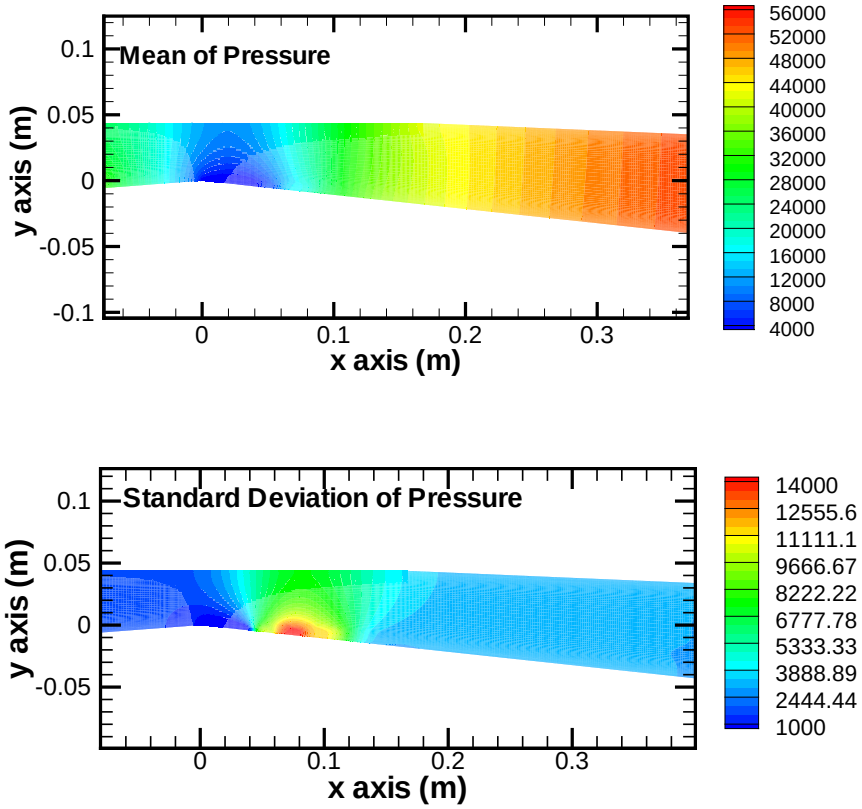

Figure 10: Contour of mean (top) and variance (bottom) of the pressure in the flowfield. The whole set of uncertainties is taken into account.

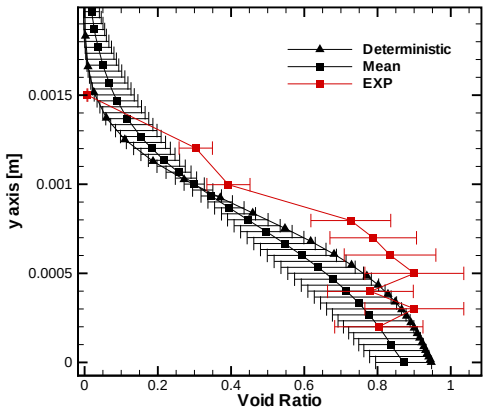

(a) Station 1

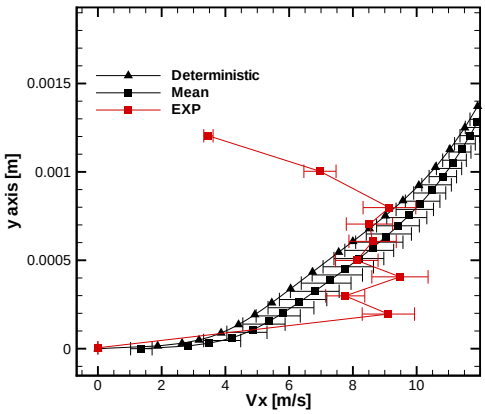

(b) Station 1

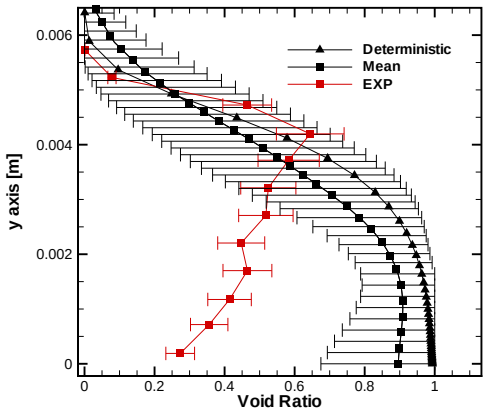

(c) Station 3

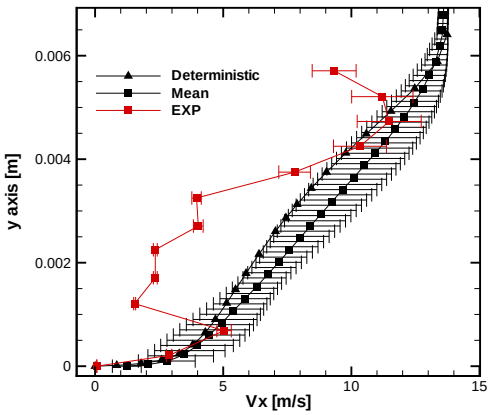

(d) Station 3

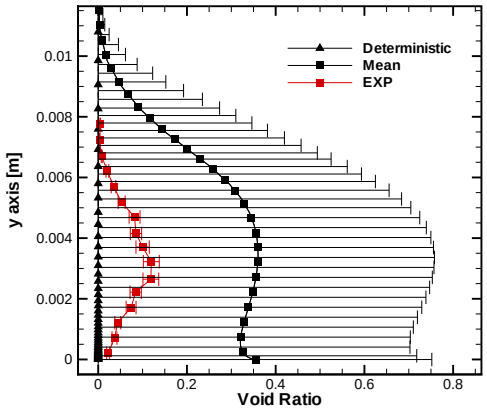

(e) Station 5

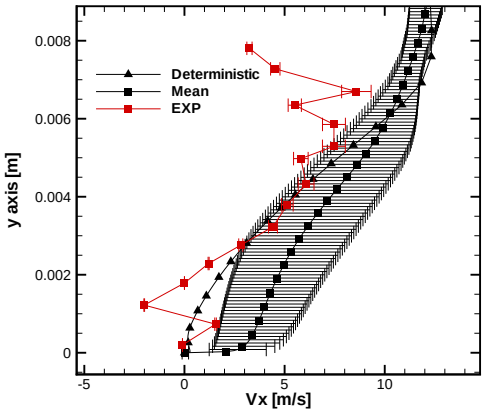

(f) Station 5

Figure 11: Radial vapor (a,c,e) and velocity (b,d,f) distributions with error bars at different sections. The whole set of incertainties is taken into account. The results are compared with experimental measurements

References

[1] A. Hosangadi and V. Ahuja. A numerical study of cavitation in cryogenic fluids, part ii: New unsteady model for dense cloud formation. In *Proceedings of the 6th International Symposium on Cavitation*, Wageningen, The Netherlands, 2006. Proceedings of the 6th International Symposium on Cavitation.

[2] J. P. Franc and C. Pellone. Analysis of thermal effects in a cavitating inducer using rayleigh equation. *Journal of Fluids Engineering*, 129:974–983, 2007.

[3] E. Goncalves and R. F. Patella. Numerical simulation of cavitating flows with homogeneous models. *Computers & Fluids*, 38:1682–1696, 2009.

[4] Y. Utturkar, J. Wu, G. Wang, and W. Shyy. Recent progress in modeling of cryogenic cavitation for liquid rocket propulsion. *Prog. Aerospace Sci.*, 41(7):558–608, 2005.

[5] R. G. Ghanem and S. D. Spanos. *Stochastic Finite Elements : a Spectral Approach*. Springer Verlag, 1991.

[6] D. Xiu and G. E. Karniadakis. The wiener-askey polynomial chaos for stochastic differential equations. *Journal of Science Computing*, 26, 2002.

[7] I. Babuska, R. Tempone, and G.E. Zouraris. Galerkin finite elements approximation of stochastic finite elements. *SIAM J. Numer. Anal.*, 42:800–825, 2004.

[8] P.G. Constantine, D.F. Gleich, and G. Iaccarino. Spectral methods for parameterized matrix equations. *SIAM J. Matrix Anal. A.*, 31:2681–2699, 2010.

[9] O.P. Le Maitre, O.M. Knio, H.N. Najm, and R.G. Ghanem. A stochastic projection method for fluid flow, i: Basic formulation. *J. Comput. Phys.*, 173:481–511, 2001.

[10] O.P. Le Maitre, M.T. Reagan, H.N. Najm, R.G. Ghanem, and O.M. Knio. A stochastic projection method for fluid flow, . ii. random process. *J. Comput. Phys.*, 181:9–44, 2002.

[11] M.T. Reagan, H.N. Najm, R.G. Ghanem, and O.M. Knio. Uncertainty quantification in reacting-flow simulations through non-intrusive spectral projection. *Combust. Flame*, 132:545–555, 2003.

[12] Thierry Crestaux, Olivier Le Maître, and Jean-Marc Martinez. Polynomial chaos expansion for sensitivity analysis. *Reliability Engineering & System Safety*, 94(7):1161–1172, 2009.

[13] P. M. Congedo, C. Corre, and J.-M. Martinez. Shape optimization of an airfoil in a bzt flow with multiple-source uncertainties. *Computer Methods in Applied Mechanics and Engineering*, 200(1):216–232, 2011.

[14] S. Li, Z. G. Zuo, and S. C. Li. Stochastic study of cavitation bubbles near boundary wall. *Journal of Hydrodynamics*, 18(3):487–491, 2006.

[15] S. J. Fariborza, D. G. Harlowa, and T. J. Delpha. Intergranular creep cavitation with time-discrete stochastic nucleation. *Acta Metallurgica*, 34(7):1433–1441, 1986.

[16] E. Giannadakis, D. Papoulias, M. Gavaises, C. Arcoumanis, C. Soteriou, and W. Tang. Evaluation of the predictive capability of diesel nozzle cavitation models. In *Proceedings of SAE International Congress*, Detroit, 2007.

[17] S. K. Mishra, K. Sudib, P. A. Deymier, K. Muralidharan, G. Frantziskonis, S. Pannala, and S. Simunovic. Modeling the coupling of reaction kinetics and hydrodynamics in a collapsing cavity. *Ultrasonics Sonochemistry*, 17(1):258–265, 2010.

[18] L. Wilczynski. Stochastic modeling of cavitation phenomena in turbulent flow. *Advances in Fluid Mechanics III*, 29:1–10, 2000.

[19] T. Goel, S. Thakur, R. T. Haftka, W. Shyy, and J. Zhao. Surrogate model-based strategy for cryogenic cavitation model validation and sensitivity evaluation. *Int. J. Numer. Meth. Fluids*, 58:969–1007, 2008.

[20] B. E. Launder and D. B. Spalding. *Lectures in Mathematical Models of Turbulence*. Academic Press, London, 1972.

[21] B. E. Launder and D. B. Spalding. The numerical computation of turbulent flows. *Computer Methods in Applied Mechanics and Engineering*, 3:269–289, 1974.

[22] G. H. Schnerr and J. Sauer. Physical and numerical modeling of unsteady cavitation dynamics. In *Fourth International Conference on Multiphase Flow*, New Orleans, USA, 2001. Fourth International Conference on Multiphase Flow.

[23] W. Yuan, J. Sauer, and G. H. Schnerr. Modeling and computation of unsteady cavitation flows in injection nozzles. *Mecanique & Industries*, 2:383–394, 2001.

[24] C. E. Brennen. *Cavitation and Bubble Dynamic*. Oxford University Press, 1995.

[25] S. Barre, J. Rolland, G. Boitel, E. Goncalves, and R. Fortes-Patella. Experiments and modelling of cavitating ïňĆows in venturi: attached sheet cavitation. *European Journal of Mechanics B/Fluids*, 28(1):444–464, 2009.

[26] B. Stutz and J.-L. Reboud. Two-phase flow structure of sheet cavitation. *Physics of Fluids*, 9(3678):1–12, 1997.

[27] P. J. Roache. *Verification and Validation in Computational Science and Engineering*. Hermosa, 1998.

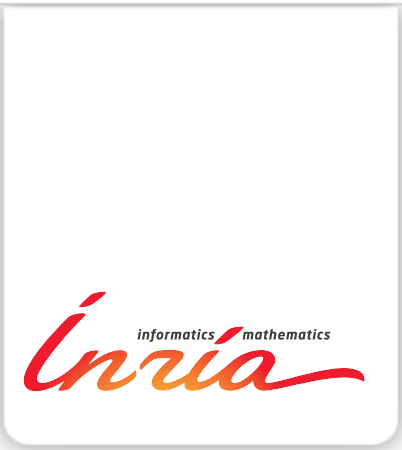

RESEARCH CENTRE
BORDEAUX – SUD-OUEST

351, Cours de la Libération
Bâtiment A 29
33405 Talence Cedex

Publisher
Inria
Domaine de Voluceau - Rocquencourt
BP 105 - 78153 Le Chesnay Cedex
inria.fr

ISSN 0249-6399